Spin transition and relaxation dynamics coupled to a crystallographic phase transition in a polymeric iron(II) spin-crossover system

Krivokapic, Itana; Enachescu, Cristian; Bronisz, Robert; Hauser, Andreas

How to cite

KRIVOKAPIC, Itana et al. Spin transition and relaxation dynamics coupled to a crystallographic phase transition in a polymeric iron(II) spin-crossover system. In: Chemical physics letters, 2008, vol. 455, n° 4-6, p. 192–196. doi: 10.1016/j.cplett.2008.02.088

This publication URL: https://archive-ouverte.unige.ch/unige:74
Publication DOI: 10.1016/j.cplett.2008.02.088

Chemical Physics Letters 455 (2008) 192–196

Contents lists available at ScienceDirect

Chemical Physics Letters

journal homepage: www.elsevier.com/locate/cplett

Spin transition and relaxation dynamics coupled to a crystallographic phase transition in a polymeric iron(II) spin-crossover system

Itana Krivokapic [a], Cristian Enachescu [b], Robert Bronisz [c], Andreas Hauser [a,*]

[a] Département de chimie physique, Université de Genève, 30, quai Ernest-Ansermet, 1211 Genève 4, Switzerland
[b] Department of Physics, Al. I. Cuza University, 700506 Iasi, Romania
[c] Faculty of Chemistry, University of Wroclaw, F. Joliot-Curie 14, 50-383 Wroclaw, Poland

ARTICLE INFO

Article history:
Received 15 November 2007
In final form 26 February 2008
Available online 2 March 2008

ABSTRACT

The spin-crossover compound $[Fe(bbtr)_3](ClO_4)_2$ (bbtr = 1,4-di(1,2,3-triazol-1-yl)butane) forms a polymeric hexagonal sheet structure. It shows an abrupt thermal spin transition with 13 K wide hysteresis around 105 K, as evidenced by single crystal optical spectroscopy. The transition temperature for the thermal high-spin→low-spin transition on cooling as well as the relaxation kinetics just below $T_c^{\downarrow}$ depend upon the history of the sample. This is typical for a nucleation and growth mechanism and domain formation. In contrast, the high-spin→low-spin relaxation following the light-induced population of the high-spin state at low temperatures is governed by the intersystem crossing process.

1. Introduction

The phenomenon of spin-crossover in transition metal complexes [1] has been and remains a topical subject due to the fact that such complexes can be switched thermally, optically and by application of pressure between the low-spin (LS) state with a maximum number of d electrons paired up in the t_{2g} sub-shell and the high-spin (HS) state with the electrons occupying the d orbitals according to Hund's rule. Upon spin-crossover, the physical properties such as magnetic and optical properties change quite dramatically. The to date hypothetical application of such systems in data processing [2], sensing [3], and displays [4] resides in the fact that cooperative effects of an elastic nature [5], due to a large bond length difference between the two states [6], may lead to thermal [3] and light-induced hysteresis [7] behaviour, and thus convey a memory effect to these systems. With iron(II) as central ion, the thermal spin transition occurs from the low-spin $^1A_1(t_{2g}^6)$ state at low temperatures to the high-spin $^5T_2(t_{2g}^4e_g^2)$ state at high temperatures. In a number of iron(II) spin-crossover systems, the HS state can be populated as long-lived metastable state well below the thermal transition temperature through light irradiation or temperature quenching. The former effect, known as light-induced excited spin state trapping (LIESST) [8], is potentially interesting for data storage and processing [2].

Recently, a new two-dimensional (2D) coordination polymer, namely $[Fe(bbtr)_3](ClO_4)_2$, has been reported by Bronisz [9]. In this compound the triazole based ligand bbtr = 1,4-di(1,2,3-triazol-1-yl)butane acts as bridging ligand between two neighbouring iron(II) centres, each of which is surrounded by six ligands. This forms a hexagonal sheet structure with the perchlorate anions in between the layers. At room temperature the space group is $P\bar{3}$, and all iron centres are crystallographically equivalent. The system presents a rare example of a (3,6) network topology [10], and it shows a very abrupt thermal spin transition in the vicinity of 105 K, which is accompanied by a hysteresis loop of some 13 K. A determination of the crystal structure in the LS state has not been possible to date, as a first order crystallographic phase transition accompanying the spin transition introduces a high degree of disorder. In the present Letter we discuss the thermal spin transition of the title compound, and we show that the transition temperature as well as the relaxation kinetics of the crystallographic phase transition depend strongly on the history of the system. We associate this with nucleation and domain formation processes. For comparison, we present the classical HS→LS relaxation following the light-induced population of the HS state from 50 K all the way up the thermal transition temperature.

2. Experimental

The experimental data presented in this paper were obtained from optical absorption measurements on single crystals. The $[Fe(bbtr)_3](ClO_4)_2$ crystals are hexagonal with well developed faces (maximum size $\sim 0.2 \times 0.2 \times 0.2\ mm^3$, see reference [9] for a detailed account of the synthesis and crystal growth, the crystals used in the present study stem from the same batch). In analogy to other spin-crossover compounds with the tetrazole and triazole coordination motifs, they are colourless at room temperature and dark red at lower temperature. They cleave easily perpendicular to the *c*-axis. For the optical spectroscopy, crystals cleaved to

* Corresponding author.
E-mail address: andreas.hauser@chiphy.unige.ch (A. Hauser).

0009-2614/$ - see front matter © 2008 Elsevier B.V. All rights reserved.
doi:10.1016/j.cplett.2008.02.088

approximately 60 μm thickness were mounted on a small aperture in a copper sample holder. For temperature dependant measurements between cryogenic and room temperature, the sample holder was inserted into a closed cycle cryostat capable of achieving temperatures down to 4 K (Janis Research) and equipped with a programmable temperature controller allowing variable temperature scans. For irradiation experiments involving LIESST, the light of a continuous Ar/Kr mixed gas laser at 488 nm (Spectra Physics 2018) was used. With laser powers of ~10 mW/mm^2 a quantitative population of the HS state was achieved in <30 s. Full absorption spectra between 9000 and 28 000 cm^{-1} (400–900 nm) were recorded on a Fourier transform spectrometer (Bruker IFS66) equipped with the respective beam splitters and detectors. Kinetic experiments at fixed temperatures were performed on a home-built system consisting of a 0.28 m spectrometer (Spex 280M) equipped with a CCD camera (Jobin-Yvon Spex CCD 3500) and polychromatic light from a 50 W tungsten halogen source as probe beam, allowing to record a full spectrum between 10 000 and 25 000 cm^{-1} at given time intervals. As the CCD camera is very sensitive, the light from the tungsten halogen lamp was attenuated to 2% of its full intensity with corresponding grey filters. As a full spectrum only takes a fraction of a second to record, and as the probe beam was gated with a shutter in parallel to the shutter of the CCD, the irradiation intensity from the probe beam is negligible with regard to the light-induced spin transition. For both the temperature dependent absorption spectra as well as the time dependent spectra, the fraction of complexes in the HS state can be extracted from the relative intensities of the typical absorption bands of the HS and the LS species [11]. By recording full spectra, artefacts due to baseline shifts from variations in diffuse scattering can be eliminated.

3. Results and discussion

The single crystal absorption spectra of $[Fe(bbtr)_3](ClO_4)_2$ shown in Fig. 1 were recorded with the light propagating along the *c*-axis. Above 110 K the spectrum presents the typical near infrared band of the HS species centred at 12 000 cm^{-1} (830 nm, $\varepsilon = 3.0$ l mol^{-1} cm^{-1}) corresponding to the $^5T_2 \rightarrow {}^5E$ ligand-field transition. At 120 K the spectrum still consists of this one band, slightly blue shifted as is normal for spin-allowed d–d transitions on lowering the temperature [12]. The spectrum recorded at 105.2 K on cooling is identical to the spectrum at 120 K. Below 100 K the band in the near infrared disappears abruptly. As exemplified by the spectrum recorded at 90.1 K, it is replaced by the more intense LS band in the visible at 18 000 cm^{-1} (590 nm, $\varepsilon = 37$ l mol^{-1} cm^{-1}), which corresponds to the $^1A_1 \rightarrow {}^1T_1$ ligand-field transition. The spectrum at 12.5 K is identical to the 90.1 K spectrum. The fact that the intensity of the HS disappears completely indicates that the spin transition is likewise complete, with no remnant HS fraction at low temperature. On heating the low-temperature spectrum is still observed at 105.2 K, and indeed it persists up to 113 K. Above that temperature it reverts abruptly to the typical HS spectrum.

As mentioned in the experimental section, the thermal transition of a single crystal can be followed quantitatively by optical spectroscopy, the LS fraction being directly proportional the area the $^1A_1 \rightarrow {}^1T_1$ ligand-field band normalised to the low-temperature spectrum [11]. Fig. 2 shows the corresponding HS fraction, γ_{HS}, as a function of temperature, obtained using different temperature sweep rates and after different thermal treatments of the system. Basically, these transition curves all are in agreement with the published curve as determined from magnetic susceptibility measurements on a polycrystalline powder [9], that is, they show a hysteresis of approximately 13 K with $T_c^{\downarrow} \approx 100$ K and $T_c^{\uparrow} \approx 113$ K indicating a first order phase transition. However, there are some characteristic differences to the powder measurements: (i) the transitions for the single crystal are much more abrupt, that is, they occur within a temperature range of <1 K, (ii) the hysteresis width depends on the temperature sweep rate, indicating that the kinetics of the phase transition are quite slow, and (iii) the apparent transition temperature for the HS→LS transition at a given temperature sweep rate depends upon the history of the crystal: when starting from room temperature (full lines in Fig. 2), the

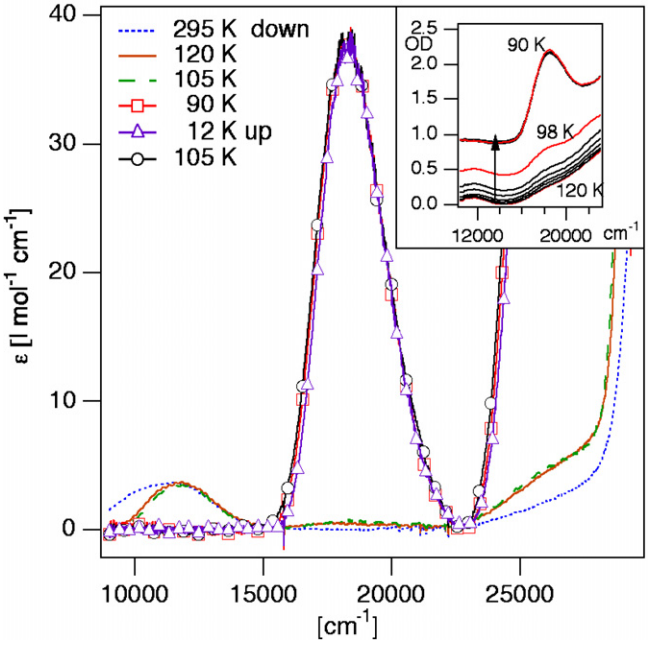

Fig. 1. Single crystal absorption spectra of $[Fe(bbtr)_3](ClO_4)_2$ at various temperatures on cooling and on heating. Inset: baseline shift during thermal transition on cooling down from room temperature due to an increase in diffuse scattering by the single crystal, the crystal goes through the phase transition.

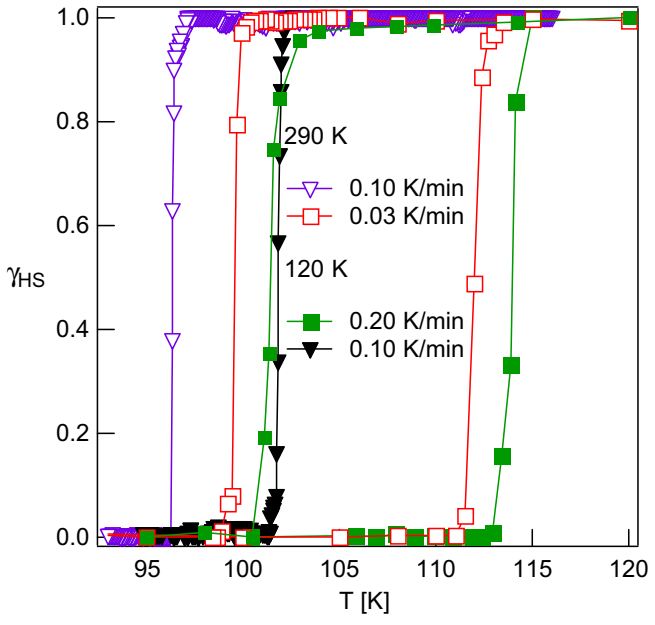

Fig. 2. The thermal spin transitions of a single crystal of $[Fe(bbtr)_3](ClO_4)_2$ for different temperature sweep rates and starting temperatures. For coming from RT, $T_c^{\downarrow} = 97$ K, whereas $T_c^{\downarrow} \approx 103$ K for coming from 120 K. $T_c^{\uparrow}$ is the same, at about 113 K.

apparent transition temperature for the HS→LS transition is lower than when coming from below the thermal transition, heating up to 120 K and then decreasing the temperature again (dotted lines in Fig. 2). Thus, at a sweep rate of 0.1 K/min, $T_c^{\downarrow} \approx 97$ K when coming from room temperature and 103 K when coming from 120 K following the first cycle. This behaviour is reproducible, that is, on taking the same crystal to room temperature and back down to below the transition temperature, $T_c^{\downarrow}$ is again ~97 K. The LS→HS transition temperature, $T_c^{\uparrow}$, remains the same at about 113 K. This behaviour can be related (i) to the inability to determine the crystal structure of the compound below the transition temperature, and (ii) to the observed substantial increase in diffuse scattering by the single crystal at the transition temperature on the first transition when coming from room temperature, as is indicated by the baseline shift in the absorption spectra in the inset of Fig. 1. On the subsequent heating to 120 K and renewed cooling cycle, this baseline shift is much less dramatic. Taken altogether, this indicates that the first spin transition on cooling from room temperature triggers a crystallographic phase transition from the high-temperature phase to a low-temperature phase with domain formation and possibly a high degree of disorder. On heating, this crystallographic low-temperature phase with its domain structure then persists to above the thermal spin transition temperature. In order to anneal the crystal back to the high-temperature phase it has to be heated all the way up to above 200 K.

The experiment was repeated using different crystals. Whereas $T_c^{\downarrow}$ of the thermal spin transition for the crystallographic low-temperature phase was 102 K and $T_c^{\uparrow}$ was 113 K for all crystals, $T_c^{\downarrow}$ from the high-temperature phase varied in the range of 92–97 K. This spread of $T_c^{\downarrow}$ from the high-temperature phase can be related to the nucleation process, which depends upon crystal quality and which is therefore characteristic for every crystal. Consequently, the differences appear only in the first transition, when the domains are actually formed and not later on when the domains already exist.

The above is supported by the two series of relaxation curves shown in Fig. 3, which were obtained following two different procedures: (a) the crystal was cooled down from room temperature to a given temperature slightly below $T_c^{\downarrow}$ and (b) the crystal was cooled to a given temperature below $T_c^{\downarrow}$ from 120 K, after having been cooled down to below $T_c^{\downarrow}$ at least once previously. The kinetics of the phase transition were followed by monitoring the LS fraction as function of time at the given temperatures. Note that these lattice relaxation curves are not to be confused with the HS→LS relaxation following the light-induced population of the HS state at low temperature, which will be discussed below. Rather, they correspond to the kinetics of the spontaneous thermal spin transition, and opposite to the classical relaxation, which becomes faster with increasing temperature, they are slower at higher temperatures, that is, closer to the transition temperature. This is in line with a first order phase transition [13]. The most striking aspect of the curves in Fig. 3 is the big difference in shape for the two different procedures. Thus, when coming down from room temperature, that is, from the high-temperature phase, the relaxation begins very slowly and then accelerates very rapidly in a sigmoidal fashion. This behaviour is typical for a nucleation and growth mechanism with the formation of domains. The relaxation curves for cooling from 120 K only, that is, from the non-annealed low-temperature phase, are much closer to single exponential. Thus, they correspond to the stochastic relaxation of more or less independent domains as a result of the non-annealed domain structure. In conclusion, around the thermal spin transition, the relaxation kinetics are governed by the kinetics of the crystallographic phase transition, which depend upon the history of the crystal.

In comparison to the relaxation curves of the crystallographic phase transition around the thermal spin transition, the more classical HS→LS relaxation curves shown in Fig. 4 can be obtained for temperatures between 50 K and 100 K. They were recorded after the quantitative, light-induced population of the HS state at 10 K and quick warming to the target temperature. As observed for a number of similar compounds [14,15], the relaxation curves are sigmoidal, confirming the cooperative character of the spin transition in the title compound. A least squares fit of the relaxation curve using the mean-field master equation with $k = k_0 \exp(\alpha\gamma_{LS})$ [14] gives a value close to 6 for the cooperativity parameter α at 50 K, similar to the related spin-crossover system $[Fe(ptz)_6](BF_4)_2$

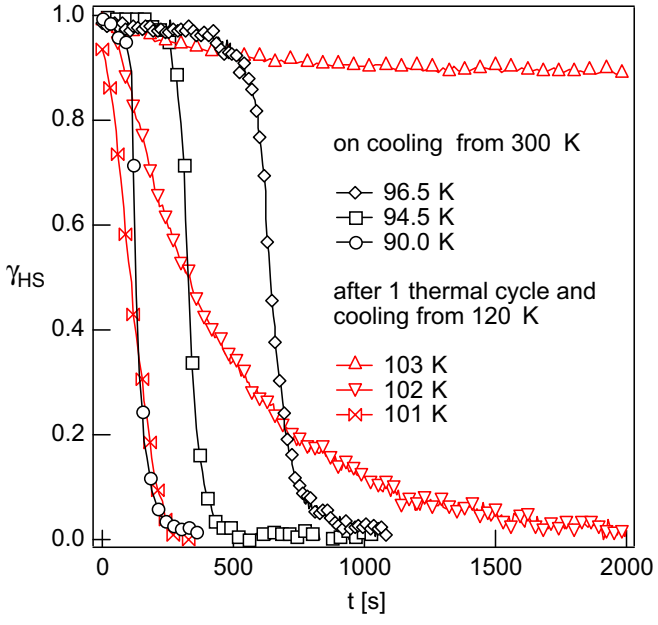

Fig. 3. Relaxation curves for a $[Fe(bbtr)_3](ClO_4)_2$ single crystal at different temperatures when starting the experiment from room temperature (procedure a, black lines), and from 120 K (procedure b, red lines). (For interpretation to colours in this figure, the reader is referred to the web version of this paper.)

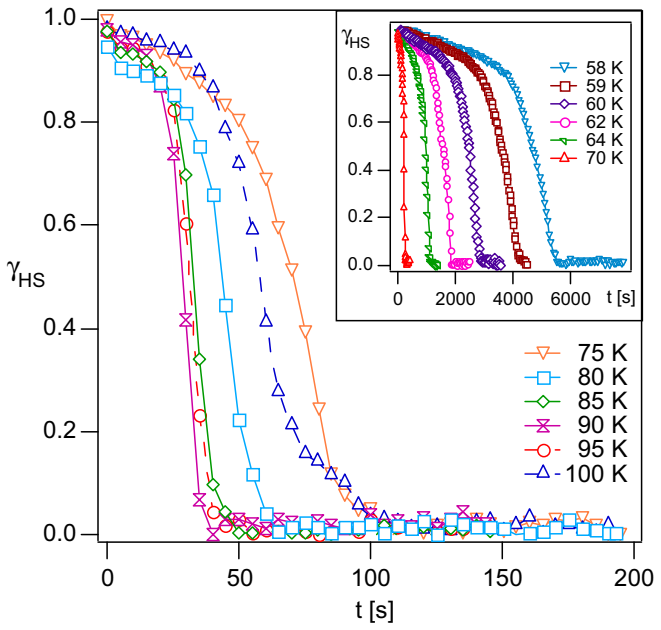

Fig. 4. HS→LS relaxation curves following a quantitative light-induced population of the HS state for temperatures between 70 and 100 K and (inset) temperatures between 58 and 70 K.

(ptz = 1-propyltetrazole) [15]. Between 50 and 90 K the relaxation process becomes faster with increasing temperature, taking more than 7 h at 50 K, only a few minutes at 70 K and 1 minute at 90 K. Between 90 and 100 K, as the thermal spin transition temperature is approached, the opposite behaviour is observed, such that at 100 K the full relaxation takes again around 2 min. This at first glance surprising behaviour is discussed in some detail below.

4. Monte Carlo simulations

In principle the HS→LS relaxation is a unimolecular process, the rate constant of which is modulated by the environment [14]. The decreasing HS→LS relaxation rate as the thermal transition temperature is approached cannot be modelled in the mean-field approximation. In order to at least qualitatively explain this somewhat unusual behaviour, a very simple 2D Ising-like system taking into account both short- and long-range interactions is treated using a Monte Carlo method. Such a system has been previously used to describe spin transition solids, considering the long-range interaction to be due to the elastic coupling mediated by the lattice as a whole and the short-range interaction to originate from the specific bonding between spin-crossover units [16].

The probability that a molecule passes from the HS state to the LS state is given by

$$W^i_{\mathrm{HS}\to\mathrm{LS}} = \frac{1}{\tau_{\mathrm{HS}\to\mathrm{LS}}}\exp\left(-\frac{E^i_a}{k_\mathrm{B}T}\right) \tag{1}$$

where $\tau_{\mathrm{HS}\to\mathrm{LS}}$ is an arbitrary time scale factor and E^i_a is the activation energy for the interacting molecule. In the normal region E^i_a can be expressed by [17]

$$E^i_a = \frac{\lambda}{4}\left(1-\frac{\Delta E^i_{\mathrm{HL}}}{\lambda}\right)^2 \approx \frac{\lambda}{4}-\frac{\Delta E^i_{\mathrm{HL}}}{2} \tag{2}$$

ΔE^i_{HL} is the energy gap between the HS and the LS state and λ the reorganisation energy. In the general case of a long-range interaction according to Spiering [5] and a short-range Ising type interaction, the energy gap for a molecule that passes from σ_i to $-\sigma_i$, ($\gamma_{\mathrm{HS}} = (1+\langle\sigma\rangle)/2$, and $\sigma_i = \pm 1$ for HS and LS, respectively) can be written as [18]

$$\Delta E_{\sigma_i\to\sigma_i} = \sigma_i(\Delta - 2\Gamma(\gamma_{\mathrm{HS}}-1/2)) - 2J\sigma_i\sum_\nu \sigma_\nu \tag{3}$$

where J and Γ are the short-and long-range interaction constants, respectively, and Δ is the energy gap between the two states in the absence of interactions. With this the transition probality can be rewritten as

$$W^i_{\mathrm{HS}\to\mathrm{LS}} = \frac{1}{\tau_{\mathrm{HS}\to LS}}\exp\left(-\frac{(\lambda/2-\Delta)+2\Gamma(\gamma_{\mathrm{HS}}-1/2)+2J\sum_\nu\sigma_\nu}{2k_\mathrm{B}T}\right) \tag{4}$$

In analogy to Eq. (1) the probability for a molecule to pass from the LS state to the HS state can be written as

$$W^i_{\mathrm{LS}\to\mathrm{HS}} = \frac{1}{\tau_{\mathrm{LS}\to\mathrm{HS}}}\exp\left(-\frac{E^{i'}_{\mathrm{HL}}}{k_\mathrm{B}T}\right) \tag{5}$$

Using as additional relation between the two transition probabilities

$$\frac{W^i_{\mathrm{LS}\to\mathrm{HS}}}{W^i_{\mathrm{HS}\to\mathrm{LS}}} = \exp\left(-\frac{\Delta G^i_{\mathrm{HL}}}{k_\mathrm{B}T}\right) = \left(-\frac{\Delta H^i_{\mathrm{HL}}}{k_\mathrm{B}T}\right)\exp\left(\frac{\Delta S^i_{\mathrm{HL}}}{k_\mathrm{B}T}\right) \tag{6}$$

the final relation for the LS→HS transition probability can be written as

$$W^i_{\mathrm{LS}\to\mathrm{HS}} = \frac{1}{\tau_{\mathrm{HS}\to\mathrm{LS}}}\exp\left(\frac{\Delta S^i_{\mathrm{HL}}}{k_\mathrm{B}}\right)\times\exp\left(-\frac{(\lambda/2+\Delta)-2\Gamma(\gamma_{\mathrm{HS}}-1/2)-2J\sum_\nu\sigma_\nu}{2k_\mathrm{B}T}\right) \tag{7}$$

With the above transition probabilities, the Monte Carlo procedure on a 3000 by 3000 2D square lattice results in the relaxation curves as a function of temperature depicted in Fig. 5. While in the absence of interactions, the probability that complex i passes from $\sigma_i = \pm 1$ to $\sigma_i = -1$ increases with increasing temperature, the short range interactions produce clusters inside the system, thus generating fluctuations that finally slow down the relaxation when the transition temperature is approached. The parameters used for the Monte Carlo simulations are in line with typical parameters for analogous spin-crossover compounds such as the effective activation energy in the absence of interactions of $\lambda/4 - \Delta/2 = 800\ \mathrm{cm}^{-1}$, the constant for the long-range interaction $\Gamma = 120\ \mathrm{cm}^{-1}$, and the entropy variation $\Delta S^0_{\mathrm{HL}} = 5\ \mathrm{cm}^{-1}\mathrm{k}^{-1}$.

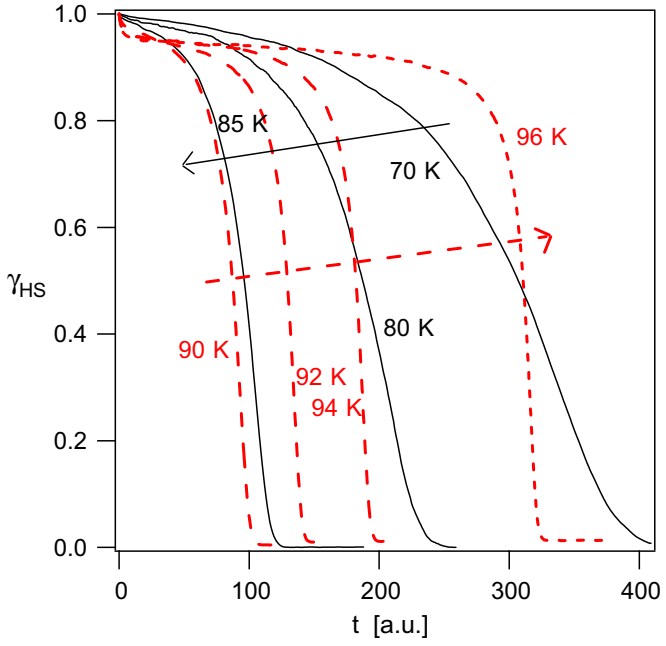

Fig. 5. Relaxation curves, calculated using a Monte Carlo method for a 2D Ising system and parameter values described in the text.

5. Conclusions

In the above, we have presented the kinetics of the thermal spin transition and the kinetics of the HS→LS relaxation following the light-induced population of the HS state on single crystals of $[Fe(bbtr)_3](ClO_4)_2$. There are two types of relaxation mechanisms, the latter being governed by the intersystem crossing process itself, the former by the crystallographic phase transition. The temperature dependence of the HS→LS relaxation as the thermal transition temperature is approached shows evidence for strong nearest-neighbour interactions, fluctuations and cluster formation.

Acknowledgements

This work was financially supported by the MAGMANet Network of Excellence of the European Union (Contract: NMP3-CT-2005-515767-2) and the Swiss National Science Foundation. C.E. thanks CNCSIS Romania for a CEEX Young Researchers Grant (1408/2006).

References

[1] P. Gütlich, H.A. Goodwin (Eds.), Spin Crossover in Transition Metal Compounds I–III, Topics in Current Chemistry, Springer, Berlin, 2004, pp. 233–235.
[2] J.F. Letard, P. Guionneau, L. Goux-Capes, Top. Curr. Chem. 235 (2004) 221.
[3] P. Gütlich, A. Hauser, H. Spiering, Angew. Chem. Int. Ed. 33 (1994) 2024.
[4] J.P. Gaudry et al., Chem. Phys. Lett. 324 (2000) 321.
[5] H. Spiering, Top. Curr. Chem. 235 (2004) 171.
[6] E. König, Prog. Inorg. Chem. 35 (1987) 527.
[7] F. Varret, K. Boukheddaden, E. Codjovi, C. Enachescu, J. Linares, Top. Curr. Chem. 234 (2004) 199.
[8] A. Hauser, Top. Curr. Chem. 234 (2004) 155.
[9] R. Bronisz, Inorg. Chem. 44 (2005) 4463.
[10] A.F. Wells, Structural Inorganic Chemistry, Clarendon Press, Oxford, England, 1984.
[11] A. Hauser, P. Gütlich, H. Spiering, Inorg. Chem. 25 (1986) 4245.
[12] J. Ferguson, Progr. Inorg. Chem. 12 (1970) 159.
[13] L.D. Landau, E.M. Lifshitz, Statistical Physics Part 1, Pergamon, 1994.
[14] A. Hauser, Chem. Phys. Lett. 192 (1992) 65.
[15] J. Jeftic, A. Hauser, J. Phys. Chem. B 101 (1997) 10262.
[16] H. Romstedt, A. Hauser, H. Spiering, J. Phys. Chem. Sol. 59 (1998) 265.
[17] R.A. Marcus, J. Chem. Phys. 43 (1965) 679.
[18] K. Boukheddaden, J. Linares, H. Spiering, F. Varret, Eur. Phys. J. B 15 (2000) 317.